

COPY of:

M. Börsch, M. Diez, B. Zimmermann, R. Reuter, P. Gräber (2002) in: "Fluorescence spectroscopy, Imaging and Probes. New Tools in Chemical, Physical and Life Sciences" (Eds. R. Kraayenhof, A.J.W.G. Visser, H.C.Gerritsen), pp. 197-207, Springer-Verlag Heidelberg (invited contribution).

**NOT FOR  
PUBLIC RELEASE**

## **Monitoring $\gamma$ -Subunit Movement in Reconstituted Single $F_0F_1$ ATP Synthase by Fluorescence Resonance Energy Transfer**

Michael Börsch, Manuel Diez, Boris Zimmermann, Rolf Reuter, Peter Gräber

Institut für Physikalische Chemie, Albert-Ludwigs-Universität Freiburg, Albertstr. 23 a, 79104 Freiburg, Germany

boersch@uni-freiburg.de

**Abstract.** The membrane-bound enzymes  $H^+$  ATP synthases contain two coupled rotary motors that drive catalysis. We applied a single molecule spectroscopy approach to monitor the internal rotation of the  $\gamma$ -subunit of the  $F_1$  part against its static counterpart, the b-subunits of the  $F_0$  part. We specifically attached two fluorophores to  $H^+$  ATP synthase from *E. coli*, namely Cy5 at the  $\gamma$ -subunit and tetramethylrhodamine at one b-subunit. After reconstitution into liposomes, these enzymes regained their full catalytic activity as measured by ATP synthesis rates. Fluorescence resonance energy transfer (FRET) was monitored in photon bursts of freely diffusing proteoliposomes using a confocal setup for single molecule detection. Incubation with non-hydrolysable AMPPNP resulted in stable intensity ratios within a photon burst. This corresponds to a fixed  $\gamma$ -subunit orientation. We detected three different FRET efficiencies, i.e.  $\gamma$ -subunit orientations. After addition of ATP a consecutive order of three distinguishable FRET efficiencies was observed within the bursts, indicating a stepwise unidirectional  $\gamma$ -subunit movement against the b-subunits.

### **1. Introduction**

$H^+$  ATP synthases ( $F_0F_1$  ATP synthases) catalyze the synthesis of ATP from ADP and inorganic phosphate in the membranes of mitochondria, chloroplasts and bacteria. Endergonic ATP synthesis is coupled to proton translocation across the membrane due to a difference in the electrochemical potential of protons. This large enzyme consists of two parts. The hydrophobic, membrane-integrated  $F_0$  part is involved in proton transport and contains subunits a,  $b_2$  and  $c_{10-12}$  for the *Escherichia coli* enzyme. The catalytic binding sites are located on the three  $\beta$ -subunits in the hydrophilic  $F_1$  part with subunit composition  $\alpha_3\beta_3\gamma\delta\epsilon$ .

Currently,  $H^+$  ATP synthase is thought to contain two rotary motors converting electrochemical energy via a mechanical form of energy to chemical energy [1]. In the  $F_0$  part proton transport across the membrane causes rotation of a ring of 10 to 12 c-subunits with respect to the non-rotating a- und b-subunits. The  $\gamma$ - and  $\epsilon$ -

subunits of the  $F_1$  part are connected to the c-ring and thus are forced to rotate within the  $\alpha_3\beta_3$  hexamer. The stepwise rotation of the  $\gamma$ -subunit induces conformational changes in the  $\beta$ -subunits, which leads to synthesis and release of ATP. According to their ADP and ATP binding affinities three different conformational states of the subunits are distinguished. The relative  $\gamma$ -subunit position determines the actual state of each  $\beta$ -subunit. Turning the  $\gamma$ -subunit in the catalytic cycle initiates cooperative sequential changes in the  $\beta$ -subunit conformations.

This enzyme can also work as a proton pump by hydrolyzing ATP. During ATP hydrolysis conformational changes of the  $\beta$ -subunits in the  $F_1$  part force the  $\gamma$ -subunit and also the ring of c-subunits in the  $F_0$  part to rotate in reverse direction. The rotating domain of the ATP synthase,  $F_1\gamma\epsilon$ - $F_0c_{10-14}$ , is called 'rotor'. The central stalk in electronmicroscopic images of the *Escherichia coli* enzyme (Fig. 1a, [2]) is therefore identified as a part of the 'rotor'. All other subunits belong to the non-rotating counterpart called 'stator'. A second stalk on the right hand side of this electronmicroscopic image in Fig. 1a probably consists of the b-subunit dimer and is part of the 'stator'.

## 2. Visualizing intersubunit rotation

ATP-driven rotation of the  $\gamma$ -subunit in isolated  $F_1$  parts of ATPases from a thermophilic bacterium was convincingly visualized by Noji et al. [3]. For this purpose, the  $F_1$  parts were attached with three His-tags onto the glass surface of microscopic coverslides. Connecting a highly fluorescent actin filament to the  $\gamma$ -subunit as a pointer, the actual orientation of this subunit with respect to the  $\alpha_3\beta_3$  hexamer was measurable by videomicroscopy at millisecond time resolution. The maximum speed of rotation depended on the length of the actin filament at high ATP concentrations. At very low ATP concentrations, rotation occurred in discrete  $120^\circ$  steps. The fluorescent actin filament method has been applied also to the  $F_1$  parts from chloroplasts and *E. coli* (see review [1]). In all cases the  $\gamma$ -subunit rotated counterclockwise during ATP hydrolysis when viewed from the membrane side to the top of  $F_1$  (see Fig. 1c, the expected sequence of  $\gamma$ -subunit orientations is  $\rightarrow A1 \rightarrow A2 \rightarrow A3 \rightarrow A1 \rightarrow$ ).

To demonstrate the rotational motion of the membrane-integrated  $F_0$  motor, a fluorescent actin filament was attached to the c-ring.  $F_0F_1$  was bound to the glass surface with His-tags. Addition of ATP resulted in rotational movement of the fluorescent actin filament [4]. High concentrations of detergent and BSA were required to prevent sticking of the filaments to the surface. However, these enzymes were not sensitive for the inhibitors generally used to show that the  $F_0F_1$  ATP synthases are coupled [5]. At enzyme concentrations in the nanomolar range used for single molecule studies treatment with detergent leads to a loss of subunits. In the case of the chloroplast  $F_1$  part, the dissociation of the  $\delta$ -subunit within minutes was detected with fluorescence correlation spectroscopy [6] (also for EF<sub>1</sub>, M.B., unpublished results). Crystallization studies of the yeast  $F_0F_1$

enzyme resulted in the loss of subunits, including the  $\alpha$ -subunit, by the use of detergent [7].

In solution, single protein dynamics can be investigated by single fluorophore detection techniques. Freely diffusing enzymes are expected not to be disturbed by interactions with surfaces. Confocal microscopy is used in combination with sensitive detectors to measure photon bursts from fluorescently labeled enzymes as they diffuse through the focal volume. If the enzymes are tagged with two different fluorophores, the conformational dynamics during catalysis can be observed by distance dependent fluorescence resonance energy transfer (FRET). The photon bursts are detected in two spectral channels and ratiometric data analysis allows for calculation of FRET efficiencies and Förster distances at a millisecond time resolution (see review [8]).

Membrane-bound enzymes like the  $H^+$  ATP synthases can be reintegrated into the membrane of lipid vesicles. These reconstituted enzymes remain fully functional for several hours even at nanomolar concentrations [9], if stored at room temperature. Determining enzyme activity as the rate of ATP synthesis is the crucial test, which requires a fully intact, coupled  $F_0F_1$  ATP synthase. These proteoliposomes diffuse freely and the detection time in the focal volume is increased by at least one order of magnitude due to slow diffusion of the vesicles (100 nm size). With a confocal detection volume of about 5.5 fl, the characteristic time of diffusion for the proteoliposomes is in the range of 30 ms as determined by fluorescence correlation spectroscopy. In photon bursts of single  $H^+$  ATP synthases with more than 500 ms duration, several turnover steps are expected during ATP hydrolysis. To monitor intersubunit rotation during catalysis, we measured relative distance changes between two amino acids - one at the 'rotor' and one at the 'stator' domain of  $F_0F_1$  - by FRET with single enzymes reconstituted into liposomes.

### 3. FRET-labeled $F_0F_1$ ATP synthase $EF_0$ -b64-TMR- $F_1$ - $\gamma$ 106-Cy5

For the FRET experiments two fluorescent labels were attached to cysteines in different subunits of  $H^+$  ATP synthase from *Escherichia coli* (Fig. 1b). The two cysteine residues were introduced by site-directed mutagenesis. We labeled  $EF_0F_1$  with Cy5 at the rotating  $\gamma$ -subunit and tetramethylrhodamine at the b-subunits. To enhance the specificity we labeled the  $\gamma$ -subunit of  $EF_1$  separately.

The cysteine mutation at the  $\gamma$ -subunit ( $\gamma$ T106C) in the  $F_1$  part is described in [10] and has been used previously for single molecule studies [11]. From this mutant only the  $F_1$  parts of the enzyme ( $EF_1$ ) were isolated [12]. The  $\gamma$ -subunit was labeled with Cy5-maleimide according to [13]. Cy5-maleimide was kindly provided by E. Schweinberger and C.A.M. Seidel (MPI für Biophysikalische Chemie, Göttingen, Germany) and H.-D. Martin (Institut für Organische Chemie und Makromolekulare Chemie, Universität Düsseldorf, Germany). The degree of labeling was determined by the corrected UV-absorption of the enzyme at 280 nm and dye absorption at 641 nm. Approximately 50 percent of the  $F_1$  parts were labeled with the FRET acceptor Cy5.  $EF_1$  was stored in liquid nitrogen.

We separately introduced cysteines in the two b-subunits belonging to the 'stator part' of the enzyme (bQ64C, to be published elsewhere). This enzyme did not carry the  $\gamma$ T106C cysteine mutation and was genetically engineered to have no other cysteines in the  $F_o$  part.  $EF_oF_1$  were isolated according to [9] and solubilized using dodecylmaltoside. The b-subunits were labeled with tetramethylrhodamine-maleimide (TMR, Molecular Probes) as FRET donor. The degree of labeling was adjusted to be in the 20 percent range to avoid double labeling, which might occur since the b-subunit in the  $F_o$  part of *E. coli* exists as a dimer (Fig. 1c). TMR-labeled  $EF_oF_1$  were reconstituted in liposomes [9] and the  $F_1$  parts were removed using a procedure adapted from [14]. TMR-labeled  $F_o$  parts, one per liposome, were reassembled with Cy5-labeled  $EF_1$  according to [15].

### 3.1 Synthesizing ATP with reconstituted $EF_o$ -b64-TMR- $F_1$ - $\gamma$ 106-Cy5

Enzyme activity was measured by the rate of ATP synthesis in an acid-base transition [17]. Labeling of the b-subunits with TMR did not affect enzyme activity. The reconstituted  $EF_o$ -b64-TMR- $F_1$  catalyzed ATP synthesis with a rate of  $60\text{ s}^{-1}$  at  $\Delta\text{pH} = 4$ . After stripping off the  $F_1$  parts, no ATP synthesis was measurable, i.e.  $F_1$  parts had been removed quantitatively. Addition of Cy5-labeled  $EF_1$  yielded a reassembled enzyme  $EF_o$ -b64-TMR- $F_1$ - $\gamma$ 106-Cy5, which synthesized ATP with rate of  $31\text{ s}^{-1}$  at  $\Delta\text{pH} = 4$ . For comparison, reassembling  $EF_o$ -b64-TMR with unlabeled  $EF_1$  resulted in a rate of  $29\text{ s}^{-1}$ . During the reassembling procedure several centrifugation steps were required to remove unbound  $EF_1$ . Centrifugation and subsequent resuspension of the proteoliposome pellet were shown to reduce the rates of ATP synthesis by up to 45 percent [17] (from  $65\text{ s}^{-1}$  to  $35\text{ s}^{-1}$ ). We conclude, that the FRET-labeled  $H^+$  ATP synthases  $EF_o$ -b64-TMR- $F_1$ - $\gamma$ 106-Cy5 are fully functional after reconstitution into liposomes.

### 3.2 Setup for single enzyme FRET analysis

FRET experiments with freely diffusing single  $H^+$  ATP synthases in liposomes were performed using a confocal setup of local design. A frequency-doubled Nd:YAG laser (532 nm, 50 mW, Coherent, Germany) was used for excitation. The circularly polarized laser beam was attenuated to 120  $\mu\text{W}$  and focussed into the liposomes containing buffer solution by a water immersion objective (UAPO 40x, N.A. 1.15, Olympus). For epi-illumination a dichroic mirror DCLP 545nm (AHF, Tübingen, Germany) was used. Out-of-focus fluorescence was filtered out by an 100  $\mu\text{m}$  pinhole (OWIS, Staufen, Germany). Fluorescence was separated into two spectral regions by a dichroic mirror DCLP 630nm (AHF, Germany). Single photons were detected with avalanche photodiodes (SPCM AQR 151, EG&G, Canada) after passing an interference filter HQ 575nm/65nm for TMR and a HQ 665nm LP for Cy5 (AHF, Germany). Photons in two channels were registered simultaneously with a PC-card (PMS 300, Becker&Hickl, Berlin, Germany).

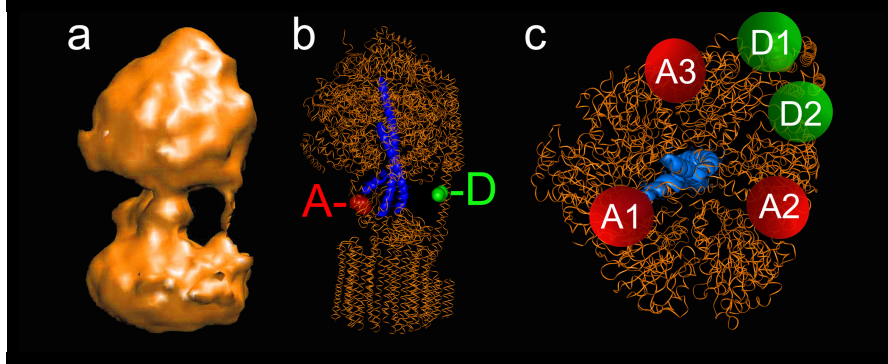


**Fig. 1.** **a)** Surface representation of electron density after three-dimensional reconstruction of electronmicroscopic images of F<sub>0</sub>F<sub>1</sub> ATP synthase from *E. coli* [2]. **b)** Modified model of EF<sub>0</sub>F<sub>1</sub> combining alignment of structural data for the  $\gamma$ - and  $\epsilon$ -subunit [18] with a homology model by S. Engelbrecht [19]. Amino acid position for the FRET donor on the b-subunit dimer is indicated with 'D', FRET acceptor position 'A' is located at the  $\gamma$ -subunit. **c)** Cross section view at the fluorophore level from the membrane side (F<sub>0</sub>) to the top of F<sub>1</sub>, showing the  $\gamma$ T106C cysteine position as 'A1' and the two bQ64C positions 'D1' and 'D2'. The distance between 'A1' and 'D1' is 7.3 nm. Counterclockwise 120° stepped rotation of the  $\gamma$ -subunit during ATP hydrolysis will approximately result in 'A2' and 'A3' positions for the  $\gamma$ T106C cysteine, respectively, in a sequence of A1→A2→A3→A1→ transitions.

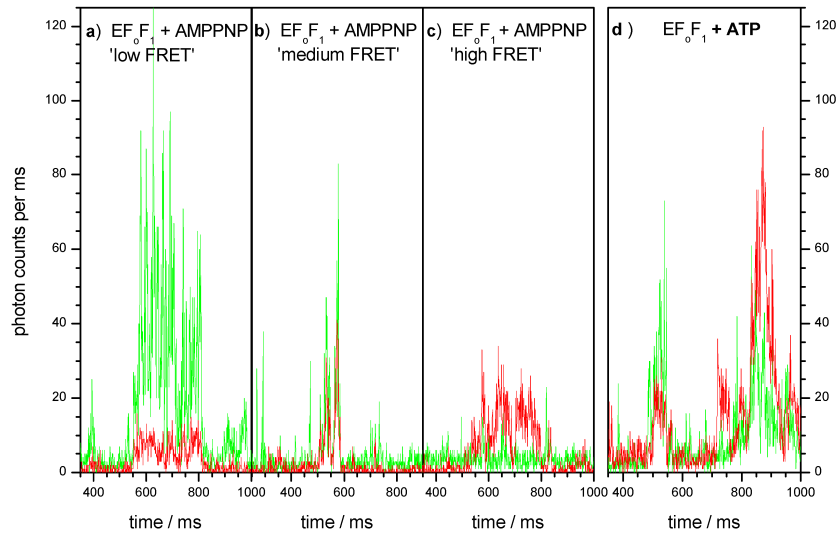


**Fig. 2.** Photon bursts of single EF<sub>0</sub>F<sub>1</sub> in liposomes. Green trace is the TMR count rate, red trace is the Cy5 count rate with 1 ms time resolution. Addition of AMPPNP (**a-c**) leads to three populations with different FRET efficiencies. The FRET donor→acceptor distance remains constant within one photon burst. **d)** Addition of ATP results in fluctuating FRET efficiencies within one photon burst.

From the fluorescence intensities  $I$  of FRET donor (green traces in Fig. 2,  $I_{(\text{Donor})}$ ) and acceptor (red traces in Fig. 2,  $I_{(\text{Acceptor})}$ ) we calculate a so-called *proximity factor*  $P$  :

$$P = I_{(\text{Acceptor})} / [ I_{(\text{Donor})} + I_{(\text{Acceptor})} ] \quad .$$

This proximity factor  $P$  allows for simple estimation of the FRET efficiency and the distance between FRET donor and acceptor. However, the value of  $P = 0.5$  corresponds to an approximated Förster radius  $R_0 = 6.5$  nm for the FRET pair TMR→Cy5 only in an ideal case, where the correction factor is 1 for the detection efficiencies of the setup and the fluorescence quantum yields [8].

For fluorescence correlation spectroscopy (FCS), the multiplexed signals were fed in parallel to a hardware autocorrelator PC-card (ALV 5000/E FAST, ALV, Langen, Germany). The actual detection volume  $V$  was calculated by FCS [11]. With a measured mean diffusion time of  $\tau_D = 350$   $\mu\text{s}$  for Rhodamine 6G in water and a translational diffusion coefficient of  $D = 2.8 \times 10^{-6}$   $\text{cm}^2 \text{s}^{-1}$  according to [16], the computed radial and axial  $1/e^2$  radii are  $\omega_0 = 0.63$   $\mu\text{m}$  and  $z_0 = 2.5$   $\mu\text{m}$ . The confocal volume is therefore  $V = \pi^{1.5} \times \omega_0^2 z_0 = 5.5$  fl.

Single enzyme FRET measurements were performed in 50 mM HEPES/NaOH buffer (pH 8.0, 2.5 mM  $\text{MgCl}_2$ ). Fluorescent impurities in the buffer solutions were removed by activated charcoal granula (Merck, Germany) with subsequent sterile filtration (200 nm pore size). ATP and AMPPNP were obtained from Böhringer (Mannheim, Germany). The ATP concentrations were held constant by a biochemical ATP regeneration kit containing 2.5 mM phosphoenolpyruvate, 10 mM KCl and 18 units/ml pyruvate kinase.

### 3.3 Discrimination of three $\gamma$ -subunit positions with AMPPNP

The orientation of the  $\gamma$ -subunit with respect to the b-subunits in the reassembled holoenzyme is not known. During the isolation procedure of  $\text{EF}_1$  most of the bound nucleotides - ATP or ADP - are lost. The conformations of all three  $\beta$ -subunits under these conditions are presumably in the 'open state' and the  $\gamma$ -subunit can wobble within the  $\alpha_3\beta_3$  hexamer due to Brownian motion. By adding AMPPNP - a non-hydrolysable ATP derivative - the position of the  $\gamma$ -subunit is fixed. The mitochondrial  $\text{F}_1$  part [20] and the yeast  $\text{F}_0\text{F}_1$  enzyme, which were crystallized in the presence of AMPPNP, showed well defined  $\gamma$ -subunit orientations [7].

We incubated the reconstituted FRET-labeled  $\text{H}^+$  ATP synthases with 1 mM AMPPNP and diluted the proteoliposomes to a final concentration below 1 nM. In the well separated photon bursts of  $\text{EF}_0\text{-b64-TMR-F}_1\text{-}\gamma 106\text{-Cy5}$  three different classes of FRET efficiencies were found (Fig. 2 a-c). Within one photon burst the mean proximity factor  $P$  remained constant.

In Fig. 2a the proximity factor  $P = 0.19$  was calculated for the photon burst starting at  $t = 550$  ms. The standard deviation was  $\text{sd} = \pm 0.11$  within this burst. This was a so-called 'low FRET' case and most probably represented the A1 position of the  $\gamma$ -subunit in Fig. 1c. To ensure the existence of FRET in this case, we compared this proximity factor with the appropriate intensity ratio for a reconstituted  $\text{EF}_0\text{-b64-TMR}$  without the Cy5 label. The 'donor only'-labeled  $\text{EF}_0\text{F}_1$

exhibited an intensity ratio  $I_{\text{(Acceptor)}} / [I_{\text{(Donor)}} + I_{\text{(Acceptor)}}]$  of 0.05 (data not shown), which is significantly smaller than the lowest FRET efficiency detected.

In Fig. 2b the proximity factor was  $P = 0.45$  ( $\text{sd} = \pm 0.15$ ) for the burst starting at  $t = 510$  ms. This was a 'medium FRET' case and presumably corresponded to the A2 position of the  $\gamma$ -subunit. The signals on both detector channels decreased in parallel within the middle of the burst. Rotational correlation times of  $\text{EF}_0\text{F}_1$  within the lipid membranes have previously been determined to be in the range of 100-200  $\mu\text{s}$  [21]. The intensity fluctuations in the millisecond time range were therefore caused by translational diffusion of the proteoliposome in and out of the focal volume or were due to rotational movement of the proteoliposome.

For the photon burst starting at  $t = 540$  ms in Fig. 2c, the calculated proximity factor was  $P = 0.75$  ( $\text{sd} = \pm 0.15$ ). This was a 'high FRET' case, probably due to the A3 position with respect to a D1 position of the FRET donor.

We calculated the proximity factors of 541  $\text{F}_0\text{F}_1$  ATP synthases in the presence of AMPPNP (Fig. 3) to analyze the distribution of the three distinct FRET efficiencies observed in single photon bursts. Data registration was automated by the 'event mode' of the multichannel scaler PC-card. The enzyme concentration was further decreased and the binning time interval enlarged to 100 ms, which is the 3-fold value of the mean diffusion time of the proteoliposomes, to get the mean value of the proximity factor for every single  $\text{F}_0\text{F}_1$  ATP synthase. A minimum threshold of 500 counts per channel per 100 ms interval was applied. The proximity factor histogram showed a broad distribution from  $P = 0.1$  to 0.9. Whereas the 'low FRET' and the 'medium FRET' efficiencies seemed to be equally distributed, the 'high FRET' efficiency with  $P > 0.65$  was significantly under-represented. This could indicate a preferred orientation of the  $\gamma$ -subunit with respect to the b-subunits in the reassembled enzyme.

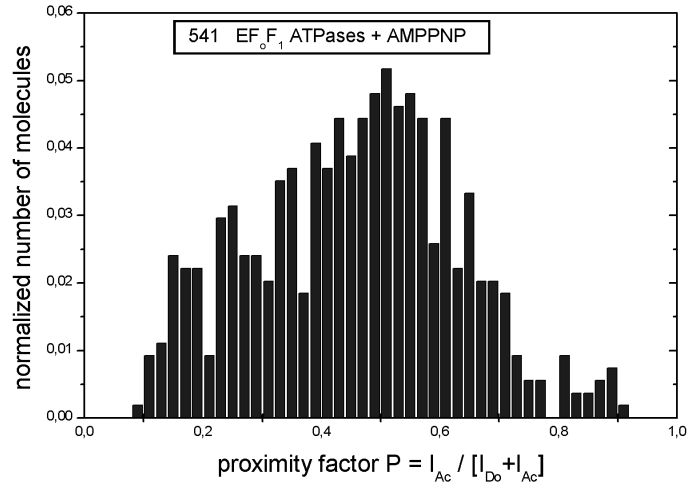


**Fig. 3.** Histogram of proximity factors  $P$  calculated from photon bursts of 541  $\text{EF}_0\text{F}_1$  in liposomes in the presence of AMPPNP. Photons were counted in 100 ms bins. Only events with more than 500 counts on both detector channels were taken for the histogram.

The FRET efficiencies were not well separated in this histogram. Intensity fluctuations due to photophysical properties of protein-bound TMR [22, 11] and photoinduced isomerization of Cy5 [23] were expected to occur in the sub-millisecond range. Also polarization effects due to rotational motion of the enzyme within the lipid membrane and the rotation of the proteoliposome itself should be averaged in a 100 ms binning time interval. In the model of EF<sub>o</sub>-b64-TMR-F<sub>1</sub>- $\gamma$ 106-Cy5 (Fig. 1c) the two possible FRET donor positions on the b-subunit dimer are indicated. Binding of TMR to D1 or D2 can result in two independent sets of Förster distances, which might slightly differ in all of the three FRET efficiencies. In principle, we should find six FRET efficiencies, but these were not resolved in the histogram. However, identification of three classes of FRET efficiencies after addition of AMPPNP was the basic prerequisite for a discrimination of all  $\gamma$ -subunit orientations during the catalytic cycle, i.e. ATP hydrolysis or synthesis.

### 3.4 Unidirectional motion of the $\gamma$ -subunit with ATP

After addition of 1 mM ATP to reconstituted EF<sub>o</sub>-b64-TMR-F<sub>1</sub>- $\gamma$ 106-Cy5 strong fluctuations of the fluorescence intensities within the photon bursts of single enzymes were measured (see Fig. 2d). This behaviour was not observed when ATP was not added. A biochemical ATP regenerating kit with phosphoenolpyruvate and pyruvate kinase was used to avoid the ADP induced inhibition of ATP hydrolysis. Due to additional fluorescent impurities the background signals were increased.

Within the photon burst starting at  $t = 482$  ms three different steps of proximity factors were distinguishable. For the first 12 ms, a mean value of  $P = 0.22 \pm 0.1$  was calculated from the FRET acceptor and donor count rates. A different value of  $P = 0.45 \pm 0.1$  was calculated starting from  $t = 494$  ms. This decreased slightly to  $P = 0.35 \pm 0.1$  after  $t = 521$  ms. In the time interval from 547 ms to 567 ms the calculated proximity factor was  $P = 0.65 \pm 0.15$ . In this photon burst the different levels of  $P$  were separated by similar decreases in intensity down to levels near the background. The sequence of proximity factors (low  $\rightarrow$  medium  $\rightarrow$  high FRET efficiency) might correspond to a sequence of  $\gamma$ -subunit positions (A1  $\rightarrow$  A2  $\rightarrow$  A3) with respect to a donor position D1 in Fig. 1c and could indicate counterclockwise rotation.

A second enzyme was observed by a photon burst starting at  $t = 715$  ms, clearly identified by the increase in the FRET acceptor count rate (red trace). In a detailed analysis we calculated  $P = 0.8 \pm 0.1$  for the first 45 ms, then the FRET acceptor count rate dropped suddenly. For the next 6 ms donor and acceptor count rates were similar at low intensities and  $P = 0.5$ . From  $t = 767$  to 786 ms the donor count rate increased and  $P = 0.3 \pm 0.1$ . The acceptor intensity rose at  $t = 790$  ms and for the next 21 ms the proximity factor fluctuated around  $P = 0.7 \pm 0.15$ . At  $t = 812$  ms the acceptor count rate dropped to the donor count rate resulting in  $P = 0.45 \pm 0.15$  for 7 ms. From  $t = 823$  to 858 ms the calculated proximity factor was  $P = 0.6 \pm 0.1$ , from  $t = 859$  to 921 ms it was  $P = 0.75 \pm 0.1$  and from  $t = 922$  to 939 ms it was  $P = 0.5 \pm 0.1$ . At  $t = 940$  ms the proximity factor dropped to  $P = 0.3 \pm 0.2$  for 20 ms. For the last 40 ms we calculated  $P = 0.65 \pm 0.15$ .

In this photon burst the expected sequence of proximity factors for the counterclockwise rotation of the  $\gamma$ -subunit was not clearly seen. The mean values for  $P$  were centered around  $P=0.8$  for 'high FRET',  $P=0.3$  for 'low FRET' and  $P=0.6$  for 'medium FRET'. Between the  $A3 \rightarrow A1$  transition we always found a proximity factor around  $P=0.6$ , which is the same as for a  $A2$  position. It remains uncertain, whether we observed a conformational substep [26] or whether the FRET donor of the enzyme was labeled at the  $D2$  position resulting in a reversed order of proximity factors during counterclockwise rotation.

The maximum ATP hydrolysis rates of reconstituted  $EF_0F_1$  range from  $200\text{ s}^{-1}$  to about  $2\text{ s}^{-1}$  depending on produced ADP concentration and the  $\Delta pH$  across the lipid membrane, which is due to proton pumping during catalysis [17]. We also found several photon bursts of other enzymes in an 'inhibited state' or with stable  $\gamma$ -subunit orientation for more than 200 ms (data not shown). The second enzyme in Fig. 2d was highly active. We identified the  $A3$  position of the  $\gamma$ -subunit by the count rate ratio as the starting point for the catalytic cycle of the enzyme. Reaching the proximity factor  $P \approx 0.8$  in the time trace indicated three turnovers or three hydrolyzed ATP. This was observed at  $t = 790, 859$  and  $960$  ms. Therefore, nine transitions were observed within 300 ms. This corresponds to a rate between  $30\text{ s}^{-1}$  and  $50\text{ s}^{-1}$ , which is the maximum rate measured in bulk ( $40\text{ s}^{-1}$  without added valinomycin and nigericin).

All time intervals observed for the transition of the  $\gamma$ -subunit positions, as identified by the changes of acceptor count rate, range from 2 to 5 ms, which is near the detection limit imposed by the 1 ms time resolution. We conclude, that the  $\gamma$ -subunit in  $EF_0F_1$  rotates stepwise during ATP hydrolysis, at least those regions of the  $\gamma$ -subunit around residue 106 with respect to the residue position 64 in the b-subunits of  $F_0$ .

#### 4 Conclusions

Labeling  $F_0F_1$  ATP synthases with two fluorophores on different subunits in combination with ratiometric single molecule FRET analysis [8] is a promising new approach to determine the orientation of the rotating  $\gamma$ -subunit. Addition of AMPPNP fixes the  $\gamma$ -subunit position and results in stable proximity factors within photon bursts of single enzymes, as they traverse the focal volume. Three different FRET efficiencies are found, which correspond to three possible orientations of the  $\gamma$ -subunit with respect to the static counterpart, the b-subunits of  $EF_0$ -b64-TMR- $F_1$ - $\gamma$ 106-Cy5.

Polarization measurements with a single fluorophore as a reporter of the actual  $\gamma$ -subunit orientation in the  $F_1$  part [24,25] require attachment of the enzyme to a surface and run into the problem of subunit dissociation. In contrast, the reconstituted  $EF_0F_1$  ATP synthases are stable at nanomolar concentrations and fully functional. Conformational dynamics are undisturbed as shown by the high ATP synthesis rates. Therefore, the fluctuations of the proximity factor  $P$  within the photon burst of one  $EF_0F_1$  ATP synthase after addition of ATP directly indicate the transitions of the  $\gamma$ -subunit orientation.

To identify conformational substeps [26] during ATP hydrolysis the time resolution has to be improved. The excitation power has to be adjusted to the photophysical limits of both fluorophores to reduce the fluctuations of the proximity factor. By analyzing the FRET donor fluorescence lifetime changes independently within the photon burst it will be possible to reduce the time resolution to 100  $\mu$ s. The time interval for the transition between two orientations of the  $\gamma$ -subunit is resolvable even for highly active enzymes. The concept of elastic power transmission between the  $F_1$  and  $F_o$  part [21] can be probed directly, because the distances of the  $\gamma$ T106C position at the  $\gamma$ -subunit and the b-subunits are measured by the FRET experiment. Finally, the ambiguity of the FRET donor position on the b-subunit dimer (D1 or D2) might be overcome by the use of a bisfunctional crosslinking fluorophore like Cy3-bis-maleimide - and the direction of  $\gamma$ -subunit rotation during ATP synthesis can be monitored.

## References

- [1] Yoshida M, Muneyuki E, Hisabori T (2001) *Nature Rev Mol Cell Biol* 2:669
- [2] Böttcher B, Bertsche I, Reuter R, Gräber P (2000) *J Mol Biol* 296:449
- [3] Noji H, Yasuda R, Yoshida M, Kinosita K (1997) *Nature* 386:299
- [4] Wada Y, Sambongi Y, Futai M (2000) *Biochim Biophys Acta* 1459:499
- [5] Tsunoda S, Aggeler R, Yoshida M, Capaldi RA (2001) *Proc Natl Acad Sci USA* 98:898
- [6] Häslér K, Pänke O, Junge W (1999) *Biochemistry* 38:13759
- [7] Stock D, Leslie AGW, Walker JE (1999) *Science* 286:1700
- [8] Deniz AA, Laurence TA, Dahan M, Chemla DS, Schultz PG, Weiss S (2001) *Annu Rev Phys Chem* 52:233
- [9] Fischer S, Gräber P (1999) *FEBS Lett* 457:327
- [10] Aggeler R, Capaldi RA (1992) *J Biol Chem* 267:21355
- [11] Börsch M, Turina P, Eggeling C, Fries JR, Seidel CAM, Labahn A, Gräber P (1998) *FEBS Lett* 437:251
- [12] Gogol EJ, Luecken U, Bork T, Capaldi RA (1989) *Biochemistry* 28:4709
- [13] Turina P, Capaldi RA (1994) *J Biol Chem* 269:13465
- [14] Löttscher HR, deJong C, Capaldi RA (1984) *Biochemistry* 23:4128
- [15] Perlin DS, Cox DN, Senior AE (1983) *J Biol Chem* 258:9793
- [16] Widengren J, Mets Ü, Rigler R (1995) *J Phys Chem* 99:13368
- [17] Fischer S, Gräber P, Turina P (2000) *J Biol Chem* 275:30157
- [18] Rodgers A, Wilce M (2000) *Nature Struct Biol* 7:1051
- [19] Engelbrecht S, <http://131.173.26.96/se/se.html>
- [20] Abrahams JP, Leslie AGW, Lutter R, Walker JE (1994) *Nature* 370:621
- [21] Junge W, Pänke O, Cherepanov DA, Gumbiowski K, Müller M, Engelbrecht S (2001) *FEBS Lett* 504:152
- [22] Wazawa T, Ishii Y, Funatsu T, Yanagida T (2000) *Biophys J* 78:1561
- [23] Widengren J, Schwille P (2000) *J Phys Chem A* 104:6416
- [24] Häslér K, Engelbrecht S, Junge W (1998) *FEBS Lett* 426:301
- [25] Adachi K, Yasuda R, Noji H, Itoh H, Harada Y, Kinosita K (2000) *Proc Natl Acad Sci USA* 97:7243
- [26] Yasuda R, Noji H, Yoshida M, Kinosita K, Itoh H (2001) *Nature* 410:898